Computer simulations of dendrimers with charged terminal groups

2006 J. Phys.: Condens. Matter 18 3581

(http://iopscience.iop.org/0953-8984/18/15/005)

INSTITUTE OF PHYSICS PUBLISHING JOURNAL OF PHYSICS: CONDENSED MATTER

J. Phys.: Condens. Matter **18** (2006) 3581–3589 doi:10.1088/0953-8984/18/15/005

Computer simulations of dendrimers with charged terminal groups

M Majtyka[1] **and J Kłos**[2]

[1] Max-Planck-Institute for Polymer Research, Postfach 3148, 55021 Mainz, Germany
[2] Faculty of Physics, A Mickiewicz University, Umultowska 85, 61-614 Poznań, Poland

Received 29 November 2005, in final form 3 March 2006
Published 30 March 2006
Online at stacks.iop.org/JPhysCM/18/3581

Abstract

Static, structural properties of dendrimers with generations ranging from $g = 3$ up to $g = 7$ with charged, monovalent terminal groups and neutralizing counterions in an athermal solvent are studied by lattice Monte Carlo simulations using the cooperative motion algorithm as the tossing scheme. The full Coulomb potential and the excluded volume interactions between pairs of ions and beads are taken explicitly into account with the reduced temperature T^* as the main, variable parameter. In particular, the influence of variation of the latter on the mean effective charge per end-bead $\langle Q \rangle$, total mean energy $\langle E \rangle$, mean-square radius of gyration $\langle R_g^2 \rangle$, and mean-square centre-to-end-bead distance $\langle R_e^2 \rangle$ is analysed and the molecular weight dependences of $\langle R_e^2 \rangle$, $\langle R_g^2 \rangle$ are shown. The simulations indicate that condensation of counterions onto the end-beads occurs as T^* is lowered. This effect is accompanied by weak, gradual swelling and shrinking of the molecules.

1. Introduction

Starburst dendrimers are macromolecules with a regular, treelike structure. They are made by cascade chemical synthesis in which, starting from the core, new branched units of monomers are attached to the so-called terminal groups [1, 2]. Such a step in the above procedure is referred to as formation of a new generation. These molecules provide a rich potential for applications in a number of fields, including industry, biomedicine, pharmacy and materials engineering. Actually, lithographic materials, nanoscale catalysts, drug delivery systems, rheology modifiers, bioadhesives, and MRI contrast agents are examples of potential applications [3].

Neutral dendrimers have been examined experimentally, analytically and numerically. For instance, the purely theoretical approaches concerning static, structural properties of dendrimers include mean-field models, self-consistent methods and Flory-type theories. Among others they provide information on such important quantities as the mean radius of gyration, dendrimer density profiles, free end distribution, scaling law for the dendrimer size, and structure factor [4–7]. Computational on- and off-lattice studies, on the other hand, involve the kinetic self-avoiding-walk algorithm, Brownian dynamics, molecular dynamics and Monte

Carlo simulations [6, 8–16]. It should also be stressed that, apart from static properties, simulations enable one to inspect the dynamical behaviour of the macromolecules. Actually, dendrimer translational self-diffusion, the size and shape fluctuations, rotational mobility, and elastic motions have been considered numerically as well [9, 17]. Experimental studies, in turn, employ for example photochemical and spectroscopic probe methods, mass spectrometry, translational diffusion and viscometry methods, scattering experiments and others [12, 18–20].

Another class of dendritic molecules is that containing charged terminal groups, i.e., branched polyelectrolytes (for example poly(amidoamine), polypropyleneimine) [21]. They have been the subject of various experimental studies using very sophisticated measurement methods. For instance, the electrophoretic mobilities of charged polypropyleneimine have been measured by capillary electrophoresis [22], the influence of the pH of the solution on the size of poly(amidoamine) has been examined with the use of small-angle neutron scattering [23], and adsorption of these molecule from solutions onto gold by a quartz crystal microbalance technique [24]. Furthermore, the lamellar structures of the cationic surfactant didodecyldimethylammonium bromide with anionic poly(amidoamine) has been investigated by small-angle x-ray scattering [25]. Such techniques as turbidimetry, dynamic light scattering, viscometry and potentiometric titration have been used in the studies of complex formations between polycations and charged dendrimers as well [26, 27].

As in the case of neutral molecules, the theoretical studies of charged dendrimers in solution with and without salt are also based on mean-field models and computer simulations. Among others, these studies have provided information on the equilibrium shape, size and structure of charged dendrimers, the monomer and counterion distribution function and the distribution of terminal groups [6, 28]. Density profiles for dendritic polyelectrolytes in solvents of various ionic strengths have also been examined by Monte Carlo simulations [29]. These simulations predict, for example, the so-called 'smart' behaviour of these molecules, i.e., a transition between 'dense core' and 'dense shell' structures of charged dendrimers as the salt concentration changes from high to low. Furthermore, by applying Monte Carlo computer simulations, possible complexes between charged dendrimers and oppositely charged polyelectrolytes have been examined [30]. Finally, the Brownian dynamics method has brought about interesting results concerning dynamic properties (self-diffusion, rotational mobility, dendrimer elastic motions, etc) of dilute solutions of charged dendrimers [17].

In this paper we carry out lattice Monte Carlo simulations of single, three-dimensional dendrimers with charged, monovalent terminal groups and their counterions without added salt. Unlike most of the previous simulation studies, we do not approximate the electrostatic interactions by the Debye–Hückel potential but take into account the Coulomb potential explicitly and concentrate on dendrimer properties with changing reduced temperature T^*. The conformations of the molecules are considered by calculating the mean-square radius of gyration $\langle R_g^2 \rangle$ and the mean-square centre-to-end-bead distance $\langle R_e^2 \rangle$. We also analyse the mean internal energy $\langle E \rangle$ of the systems and measure the condensation of counterions by means of the mean effective charge per end-bead $\langle Q \rangle$ [31–33]. These quantities are calculated by employing Monte Carlo simulations in the canonical ensemble with a version of the cooperative motion algorithm (CMA) as the tossing scheme on the face-centred cubic (fcc) lattice [34–38]. The remaining part of the paper is organized as follows. First, the simulation method and the measured quantities are defined. Then, the results of our simulations are presented and discussed. Finally, conclusions and remarks are given.

2. Model and numerical procedure

The model system consists of a single dendrimer on an fcc lattice of size L^3 with periodic boundary conditions. A dendrimer is, in turn, a treelike collection of beads connected by rigid,

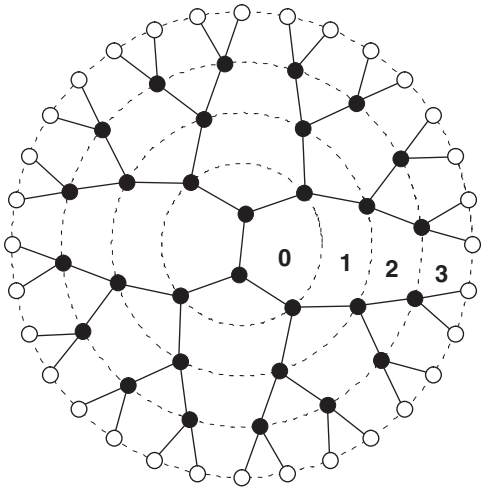

Figure 1. Schematic 2D picture of dendrimers (supplied by T Pakula).

nonbreakable bonds of length $a = u\sqrt{2}$ (where u is the length unit) so as to constitute the macromolecular skeleton (for a 2D schematic representation see figure 1). Before performing actual simulations, dendrimers with assumed generations g, spacer length $P = 1$ and branching functionality $m = 2$ are sequentially (generation after generation) formed by a growth process starting from a primary initiator. Thus, in terms of g, the total number of monomers N and terminal groups N_t are given by

$$N_t = 2^{g+2} \tag{1a}$$

$$N = 2^{g+3} - 2. \tag{1b}$$

Furthermore, in order to model a polyelectrolyte dendrimer, each end-bead is supposed to carry a unit positive electric charge, whereas N_t free beads (counterions) carry monovalent charges of the opposite sign (see figure 2). The solvent is implicitly included in the simulations by its permittivity ε.

The electrostatic interaction between pairs of charges is the total Coulomb energy

$$E(r_{ij}) = \frac{E_c(r_{ij})}{\delta} = \frac{z_i z_j}{r_{ij}}, \tag{2}$$

where r_{ij} is the distance between ions i and j, z_k is the valence of ion k ($z_k = \pm 1$), and $\delta = e^2/\varepsilon u$ is the energy unit with e denoting the electric charge. The long-range nature of the Coulomb interactions is treated by the standard Ewald summation method with the minimum image convention for the real-space term, $\kappa = 5/L$, $k_{max} = 5$ for the sum in reciprocal space and for a conducting external medium [39]. In this paper, we calculate thermodynamic averages of various quantities at the reduced temperature T^* defined as $T^* = k_B T/\delta$, where T is the absolute temperature and k_B is the Boltzmann constant. Furthermore, the excluded volume condition is also taken into account by preventing a lattice site from being occupied by more than one element. Since this is the only short-ranged interaction between the monomers, the dendrimers are in an athermal solvent.

Here, the configurations are tossed by a version of the CMA that is generalized to dendrimeric molecules. The elementary moves are classified and coded for all the local conformations of threes of bonds branching from one point. Originally, this idea was formulated for linear chains, i.e., for pairs of neighbouring bond vectors [40]. The CMA

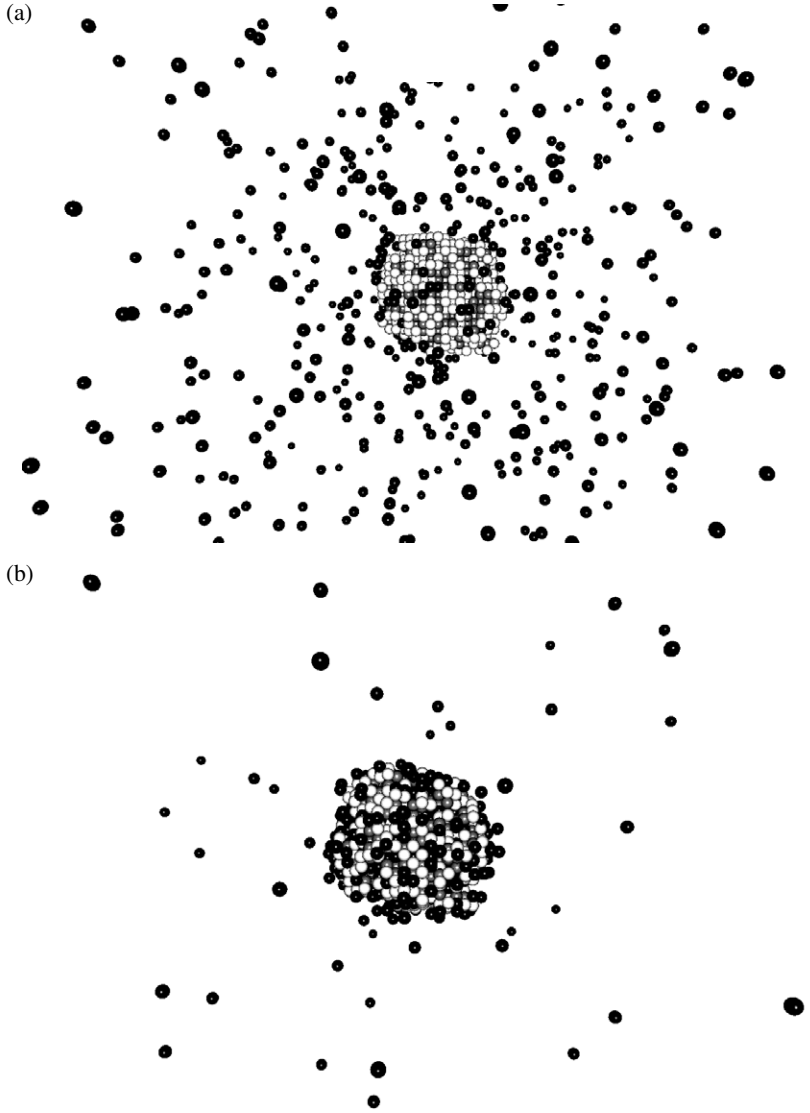

Figure 2. The configuration snapshots (in different scales) for $g = 7$ and for (a) $T^* = 10$, (b) $T^* = 0.5$. The black, grey and white spheres represent the counterions, end-beads and neutral monomers, respectively.

provides a richer combination of reconfigurations of polymers compared to the earliest lattice algorithms such as the Verdier–Stockmayer one [41]. Actually, while the latter enables only local chain configurational changes (end-bond motion, kink-jump motion and crankshaft rotation), the set of elementary moves for the former enables both local and non-local ones.

The tossing scheme used can be outlined in the following way. (1) A bead (monomer, counterion) and one of its neighbouring lattice sites are selected at random. (2) If the latter is empty an elementary CMA move is performed. In case the selected bead is a counterion it is translated to the empty site. This way another empty site (the abandoned one) is generated

which is the end of the trial reconfiguration for single, free beads. In case the selected bead is a monomer, it is moved to the empty site as well. Furthermore, depending on the local situation encountered, in order that no bonds are broken and that the sequence of beads on the dendrimer is preserved, a number of monomers that follow the selected one are also shifted collectively one after another by subsequent translating by one lattice site until an empty site is finally generated. This is the end of the trial reconfiguration for the monomers. (3) If the lattice site selected in (1) is occupied, the whole of step (1) is repeated.

The new configuration generated in such a way is accepted or rejected according to a probability of the Metropolis type [42]

$$p = \min\left[1, \exp\left(-\frac{\Delta E}{T^*}\right)\right], \tag{3}$$

with $\Delta E = E_{\text{new}} - E_{\text{old}}$ (E_{new} and E_{old} are energies after and before a random reconfiguration, $E = E_{\text{c}}/\delta$).

In the simulations, we have computed the mean-square centre-to-end-bead distance

$$\left\langle R_{\text{e}}^2 \right\rangle = \left\langle \frac{1}{N_{\text{t}}} \sum_{i=1}^{N_{\text{t}}} \left(r_{\text{e},i} - r_{\text{c}}\right)^2 \right\rangle, \tag{4a}$$

the mean-square radius of gyration

$$\left\langle R_{\text{g}}^2 \right\rangle = \left\langle \frac{1}{N} \sum_{i=1}^{N} \left(r_i - r_{\text{cm}}\right)^2 \right\rangle, \tag{4b}$$

the mean internal energy $\langle E \rangle$, and the mean effective charge per end-bead

$$\langle Q \rangle = 1 - \frac{\langle N_{\text{c}} \rangle}{N_{\text{t}}}. \tag{5}$$

$r_{\text{e},i}$, r_{c} denote the position vectors of the ith end-bead and of the initiator centre, r_i and r_{cm} of the ith monomer and of the dendrimer centre of mass, respectively. $\langle N_{\text{c}} \rangle$ is the mean number of condensed counterions (a counterion is considered condensed when it occupies a nearest-neighbour site of any end-bead), and the bracket $\langle\,\rangle$ stands for thermodynamic averaging. Finally, we have also considered the specific heat C_v calculated by using fluctuations

$$C_v \approx \frac{\left\langle E^2 \right\rangle - \langle E \rangle^2}{T^{*2}}. \tag{6}$$

The simulations have been performed on a 3D fcc lattice of size $L^3 = 80 \times 80 \times 80\ u^3$ for systems of single dendrimers with generations $g = 3, \ldots, 7$ at temperatures $T^* = 10$, 5, 2.5, 1, 0.5, 0.25, 0.1, 0.05, respectively. Mostly, configurations obtained for some T^* were initial ones for further calculations at lower T^*. The number of Monte Carlo Steps (MCSs; one Monte Carlo Step is $N + N_{\text{t}}$ trial reconfigurations) needed for the systems to reach equilibrium depended on g with the tendency to be larger for higher g.

3. Results

In order to make sure that the simulated systems have properly equilibrated at given T^* we shall start by examining the specific heat C_v [43]. Actually, for most of the considered temperatures we have found good agreement between C_v calculated by applying equation (6) and by graphical differentiation of the mean energy $\langle E \rangle$ with respect to T^* (the example for $g = 5$ is shown in figure 3(a)). This, in turn, implies that the inspected systems have reached thermodynamic equilibrium except for the two lowest temperatures $T^* = 0.05$, 0.1, where

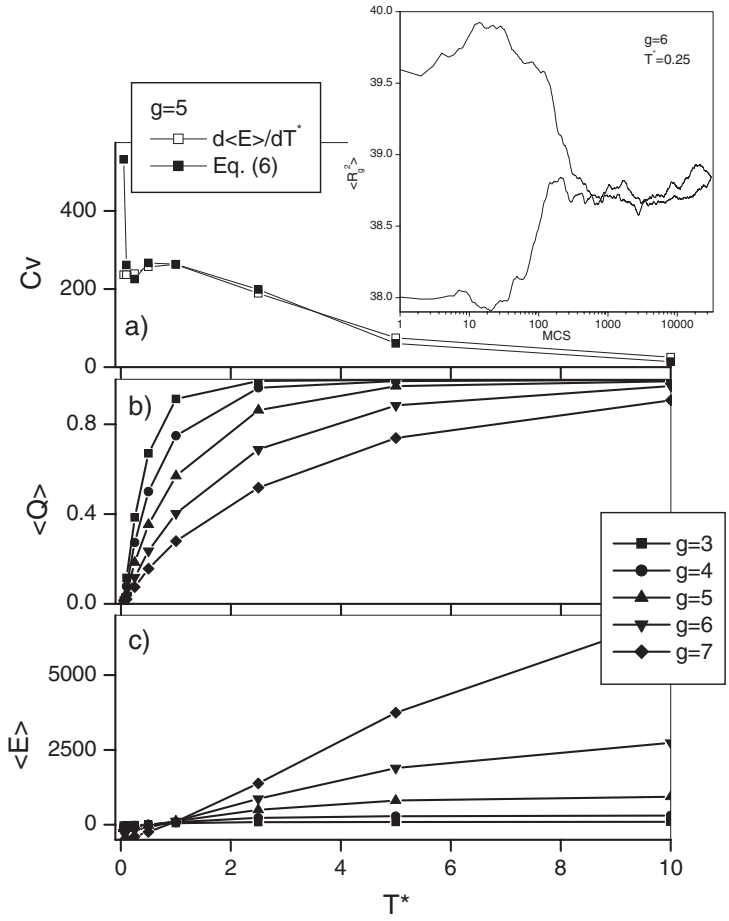

Figure 3. (a) The specific heat C_v versus T^* for $g = 5$, (b) the effective mean charge per end-bead $\langle Q \rangle$ versus T^* for $g = 3, \ldots, 7$, (c) the mean electrostatic energy $\langle E \rangle$ versus T^* for $g = 3, \ldots, 7$. The inset shows $\langle R_g^2 \rangle$ versus MCS for two different initial states for $g = 6$ and for $T^* = 0.25$.

they are more likely to be trapped in metastable states. Thus, the mean values obtained for these temperatures should be seen as averages corresponding to a single basin in the energy landscape rather than true, equilibrium values. Furthermore, the inset of figure 3 showing $\langle R_g^2 \rangle$ versus MCS for $g = 6$, $T^* = 0.25$ for two runs started from different configurations, provides an indication that convergence towards equilibrium is secured independently of the initial microstates.

In figure 3(b), the mean effective charge per end-bead $\langle Q \rangle$ is plotted versus T^*. We see that, for all the generations, $\langle Q \rangle$ monotonically decreases with temperature, i.e., the condensation phenomenon starts to appear ($\langle Q \rangle < 1$) as T^* is lowered. The drop in $\langle Q \rangle$ is very sharp for $g = 3, 4$, whereas for $g = 5, 6, 7$ it is more smooth, and the reduction in $\langle Q \rangle$ is present even at higher T^*. Furthermore, the observed tendencies are such that $\langle Q \rangle(T^*, g_1) < \langle Q \rangle(T^*, g_2)$ for $g_2 < g_1$. In other words, the reduction of dendrimer charge is better pronounced for molecules with larger generations at given T^*. At extremely low T^*, $\langle Q \rangle$ is practically zero—almost all of the counterions are condensed, and the dendrimer is electrically neutral. Qualitatively, the effect of condensation is well seen in figure 2, where

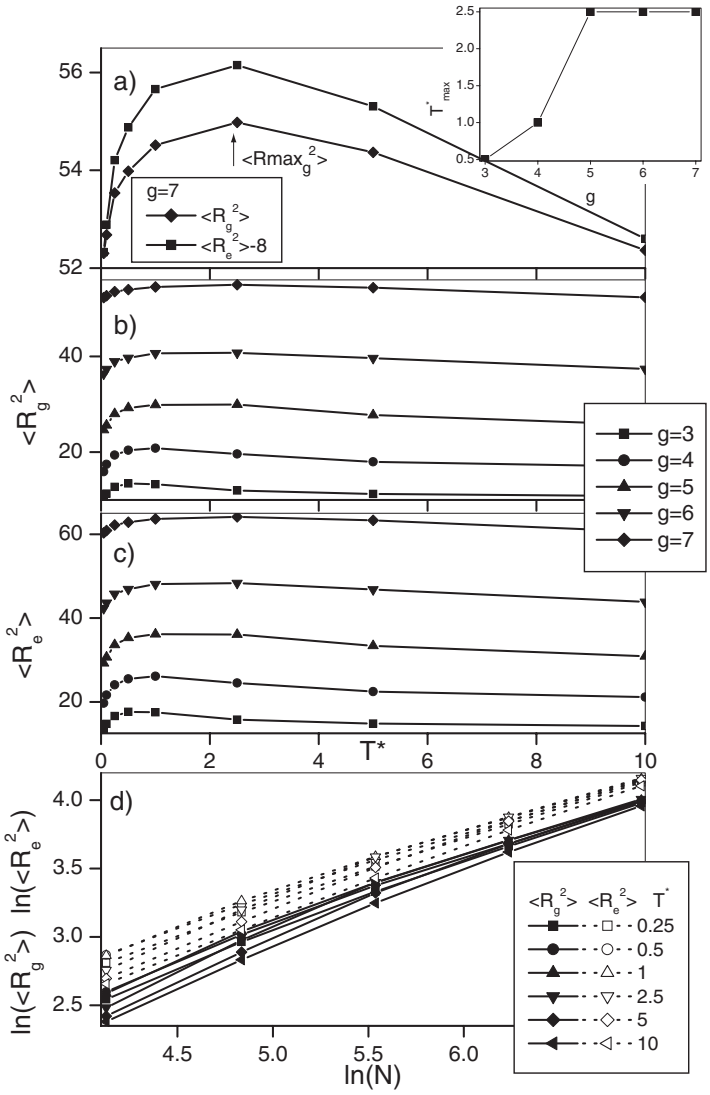

Figure 4. (a) The mean-square radius of gyration $\langle R_g^2 \rangle$ and the mean-square centre-to-end-bead distance $\langle R_e^2 \rangle$ (shifted down by eight) versus T^* for $g = 7$; the inset shows T^* at which $\langle R_g^2 \rangle$ and $\langle R_e^2 \rangle$ are maximal versus g, (b) the mean-square radius of gyration $\langle R_g^2 \rangle$ versus T^* for $g = 3, \ldots, 7$, (c) the mean-square centre-to-end-bead distance $\langle R_e^2 \rangle$ versus T^* for $g = 3, \ldots, 7$, (d) the molecular weight dependences of $\langle R_e^2 \rangle$ and $\langle R_g^2 \rangle$ at various temperatures.

representative snapshots of the dendrimer with $g = 7$ and counterions are shown for $T^* = 10$ and 0.5, respectively. Furthermore, as indicated by figure 3(c), the behaviour of $\langle Q \rangle$ is accompanied by a gradual drop in the average electrostatic energy $\langle E \rangle$.

Next, in figure 4 we inspect the dendrimer conformational changes by analysing the mean-square centre-to-end-bead distance $\langle R_e^2 \rangle$ and the mean-square radius of gyration $\langle R_g^2 \rangle$ as functions of T^*. Figure 4(a) refers to the single generation $g = 7$, whereas figures 4(b) and (c) refer to all of them. We observe that for all the considered generations, both $\langle R_e^2 \rangle$ and $\langle R_g^2 \rangle$ reach broad maxima in some intermediate temperature region where the branches of the

molecule exist in more extended forms. As indicated by the inset in the top right-hand corner of figure 4, the locations of the maxima reveal a tendency to shift towards lower T^* as g decreases. In the extremes of low and high T^*, in turn, $\langle R_e^2 \rangle$ and $\langle R_g^2 \rangle$ are reduced when compared to the temperatures in between, and the low-temperature shrinking is sharper. Our computational data indicate, however, that at least in the case of our model, the above-described changes in size are relatively weak because the parameter $\alpha = 1 - \langle R_g^2 \rangle^{1/2}(T^* = 10)/\langle R_{\max g}^2 \rangle^{1/2}$ (see figure 4(a)) varies from about 0.03 for $g = 7$ to about 0.1 for $g = 3$. The molecular weight dependences of $\langle R_g^2 \rangle$ and $\langle R_e^2 \rangle$ for various T^* are shown in figure 4(d). We do not consider them to be linear and so the scaling relations of the form $\langle R^2 \rangle \sim N^\nu$ do not seem to hold in this case.

4. Summary

In this paper, using a version of the cooperative motion algorithm, we have carried out Monte Carlo simulations of single dendrimers with charged, monovalent terminal groups and counterions at a number of reduced temperatures. Unlike most previous studies on this subject, we have examined explicitly the effect of counterions on dendrimer size and structure. The calculations have shown that, as the temperature decreases from high to low, the mean energy drops and condensation of counterions onto the dendrimers occurs. This effect is also accompanied by weak conformational changes of the molecules that gradually swell and shrink.

Acknowledgments

This work was supported by Marie Curie European Grant SIMPOL, MERG-CT-2004, Contract No 006348. The authors wish to acknowledge the Poznań Supercomputing and Networking Centre where the calculations were performed. The authors are very grateful to the late T Pakula for fruitful collaboration and to M Banaszak for helpful discussions.

References

[1] Tomalia D A, Baker H, Dewald J R, Hall M, Kallos G, Martin S, Roeck J, Ryder J and Smith P 1985 *Polym. J.* **17** 117
[2] Buhleier E W, Wehner W and Vogtle F 1978 *Synthesis* **1978** 155
[3] www.azonano.com/Details.asp?ArticleID=1142#_Dendrimers_(Organic_Nanoparticles)
[4] De Gennes P G and Hervet H 1983 *J. Phys. Lett.* **44** 251
[5] Boris D and Rubinstein M 1996 *Macromolecules* **29** 7251
[6] Timoshenko E G, Kuznetsov Y A and Connolly R 2002 *J. Chem. Phys.* **117** 9050
[7] Lyulin S V, Evers L, van der Schoot P, Darinskii A, Lyulin A V and Michels M A J 2004 *Macromolecules* **37** 3049
[8] Lescanec R L and Muthukumar M 1991 *Macromolecules* **24** 4892
[9] Karatasos K, Adolf D B and Davies G R 2001 *J. Chem. Phys.* **115** 5310
[10] Lyulin A V, Davies G R and Adolf D B 2000 *Macromolecules* **33** 6899
[11] Mansfield M L and Klushin L I 1993 *Macromolecules* **26** 4262
[12] Rathgeber S, Pakula T and Urban V 2004 *J. Chem. Phys.* **121** 3840
[13] Naylor A N, Goddard W A III, Kiefer G E and Tomalia D A 1989 *J. Am. Chem. Soc.* **111** 2339
[14] Lescanec R L and Muthukumar M 1990 *Macromolecules* **23** 2280
[15] Murat M and Grest G S 1996 *Macromolecules* **29** 1278
[16] Chen Z Y and Cui S-M 1996 *Macromolecules* **29** 7943
[17] Lyulin S V, Darinskii A A, Lyulin A V and Michels M A 2004 *Macromolecules* **37** 4676
[18] Jockusch S, Ramirez J, Sanghvi K, Nociti R, Turro N J and Tomalia D A 1999 *Macromolecules* **32** 4419
[19] Weener J W, van Dongen J L J and Meijer E W 1999 *J. Am. Chem. Soc.* **121** 10346
[20] Pavlov G M, Korneeva E V and Meijer E W 2002 *Colloid Polym. Sci.* **280** 416
[21] Kreisel J W, König S, Freitas M A, Marshall A G, Leary J A and Tilley T D 1998 *J. Am. Chem. Soc.* **120** 12207

[22] Welch C F and Hoagland D A 2003 *Langmuir* **19** 1082
[23] Nisato G, Ivkov R and Amis E J 2000 *Macromolecules* **33** 4172
[24] Rahman K M A, Durning C J, Turro N J and Tomalia D A 2000 *Langmuir* **16** 10154
[25] Li X, Imae T, Leisner D and López-Quintela M A 2002 *J. Phys. Chem.* B **106** 12170
[26] Zhang H, Dubin P L, Ray J, Manning G S, Moorefield C N and Newkome G R 1999 *J. Phys. Chem.* B **103** 2347
[27] Leisner D and Imae T 2004 *J. Phys. Chem.* B **108** 1798
[28] Govorun E N, Zeldovich K B and Khokhlov A R 2003 *Macromol. Theory Simul.* **12** 705
[29] Welch P and Muthukumar M 1998 *Macromolecules* **31** 5892
[30] Welch P and Muthukumar M 2000 *Macromolecules* **33** 6159
[31] Victor J M and Hansen J P 1987 *Europhys. Lett.* **3** 1161
[32] Takashima J, Takasu M and Hiwatari Y 1989 *Phys. Rev.* A **40** 2706
[33] Winkler R G, Gold M and Reineker P 1998 *Phys. Rev. Lett.* **80** 3731
[34] Kłos J and Pakula T 2004 *J. Chem. Phys.* **120** 2496
[35] Kłos J and Pakula T 2004 *J. Chem. Phys.* **120** 2502
[36] Kłos J and Pakula T 2005 *J. Chem. Phys.* **122** 134908
[37] Kłos J and Pakula T 2005 *J. Chem. Phys.* **123** 024903
[38] Kłos J and Pakula T 2005 *J. Phys.: Condens. Matter* **17** 5635
[39] Allen M P and Tildesley D J 1984 *Computer Simulation of Liquids* (Oxford: Clarendon)
[40] Pakula T 1991 *J. Chem. Phys.* **95** 4685
Pakula T 2004 Simulations on the completely occupied lattice *Simulation Methods for Polymers* ed M J Kotelyanskii and D N Theodorou (New York: Dekker) chapter 5
[41] Sokal A D 1995 Monte Carlo methods for the self-avoiding walk *Monte Carlo and Molecular Dynamics Simulations in Polymer Science* ed K Binder (New York: Oxford University Press) chapter 2
[42] Metropolis N, Rosenbluth A W, Rosenbluth N N, Teller A H and Teller E 1953 *J. Chem. Phys.* **21** 1087
[43] Carruzzo H M and Yu C C 2002 *Phys. Rev.* E **66** 021204